Eco-evolutionary processes underlying early warning signals of population declines

Gaurav Baruah[1], Christopher F. Clements[1,2], Arpat Ozgul[1]

[1] Department of Evolutionary Biology and Environmental studies, University of Zurich

[2] School of Biological Sciences, University of Bristol

Keywords: stability, early warning signals, population declines, eco-evolutionary factors, trait dynamics, quantitative genetics

Corresponding author: Gaurav Baruah; gaurav.baruah@ieu.uzh.ch

Abstract

1. Environmental change can impact the stability of populations and can cause rapid declines in abundance. Abundance-based warning signals have been proposed to predict such declines, but these have been shown to have limited success, leading to the development of warning signals based on the distribution of fitness-related traits such as body size.

2. The dynamics of such traits in response to external environmental perturbations are controlled by a range of underlying factors such as reproductive rate, genetic variation, and plasticity. However, it remains unknown how such ecological and evolutionary factors affect the stability landscape of populations and the detectability of abundance and trait-based warning signals of population decline.

3. Here, we apply a trait-based demographic approach and investigate both trait and population dynamics in response to gradual changes in the environment. We explore a range of ecological and evolutionary constraints under which the stability of a population may be affected.

4. We show both analytically and with model-based simulations that strength of abundance-based early warning signals is significantly affected by ecological and evolutionary factors.

5. Finally, we show that a unified approach, combining trait- and abundance-based information, significantly improves our ability to predict population declines. Our study suggests that the inclusion of trait dynamic information alongside generic warning signals should provide more accurate forecasts of the future state of biological systems.

1. Introduction

Predicting catastrophic and non-catastrophic collapses of populations and ecosystems in response to novel environmental pressures are critical if we are to mitigate the effects of global change and minimize the loss of biodiversity (Cardillo et al., 2005; Thomas et al., 2004). These collapses are however difficult to predict (Boettiger & Hastings, 2012b; Clements, Drake, Jason, & Ozgul, 2015; Clements & Ozgul, 2018). One suite of methods, which may achieve this, are early warning signals derived from dynamic systems theory (Scheffer et al., 2009b; van Nes & Scheffer, 2007). Such methods assume that a dynamical system, for example a biological population, that is under increasing continuous external pressure, will show a property called critical slowing down (CSD) as it approaches a tipping point- the point at which the system's state can substantially change in response to a slight perturbation. Around the vicinity of this tipping point, the system takes longer to return to its original state after every perturbation (Wissel, 1984; Strogatz, 1994; Scheffer *et al.*, 2009).

The occurrence of CSD is a direct implication of the dominant eigenvalue of the system approaching zero (for continuous dynamical system) (van Nes & Scheffer, 2007) or 1 (for a discrete dynamical system) (Krkoek & Drake, 2014). As a direct consequence of CSD, statistical moments embedded within abundance time-series data, particularly variance and autocorrelation will show marked increase over time. These two indicators are the prominent abundance-based statistical metrics, and, along with various other temporal (Boettiger & Hastings, 2012a; Chevalier & Grenouillet, 2018; Vasilis Dakos et al., 2012; Drake & Griffen, 2010; Jarvis, McCann, Tunney, Gellner, & Fryxell, 2016) and spatial (Butitta, Carpenter, Loken, Pace, & Stanley, 2017; Dai, Korolev, & Gore, 2013) metrics, are commonly known as early warning signals (EWS).

Changes in autocorrelation and variance are measures of the stability of a system, derived from the theory of alternative stable states (Clements & Ozgul, 2018; Wissel, 1984). Holling's (1973) fundamental work on stability and resilience laid the foundation for future work on deriving stability criteria for systems with alternative equilibrium states. Stability of a dynamical system can be characterized by the classic ball-in-cup diagram (Clements & Ozgul, 2018; Holling, 1973; Nolting & Abbott, 2015), where the 'ball' represents the state of the system and the 'cup' represents the potential energy landscape (Fig.1). The stability of the system is thus quantified by the depth of the energy landscape, and resilience by the size of the cup (Clements & Ozgul, 2018; Villa Martín, Bonachela, Levin, & Muñoz, 2015). In response to continuous exogenous pressure, the system loses resilience (for example, decline in population numbers) and the energy landscape shrinks (Fig. 1). Concurrent with the shrinkage of the landscape, there is also a decrease in the depth of the 'ball-in-cup'

73 landscape signaling a loss in stability (Fig. 1). It is this loss in stability, which
74 statistical EWSs such as variance and autocorrelation measure as an alternative for
75 loss of global resilience of the system (Clements and Ozgul 2018). The shape of the
76 ball-in-cup landscape thus determines the dynamics of the state variable in response
77 to an exogenous environmental change (Beisner, Haydon, & Cuddington, 2003).
78
79 However, the shape of the 'ball-in-cup' landscape can be changed not only by
80 exogenous pressures, but can also be altered by intrinsic factors associated with the
81 system's dynamics (Beisner et al., 2003). Changes in these intrinsic factors might
82 alter the location of an equilibrium state, or destabilize the current state, causing the
83 system to arrive at a point closer to the other alternative state (Fig. 1). For a biological
84 population, the state of the population will be characterized by its current abundance.
85 Responses of this state variable (abundance) to an exogenous environmental pressure
86 will be a combination of ecological and evolutionary responses controlled by factors
87 such as genetic variation or plasticity (Ozgul et al., 2010; Price, Qvarnström, & Irwin,
88 2003). For example, plastic responses to fluctuating changes in the exogenous
89 environment are usually fast which consequently stabilizes population fluctuations
90 (Reed, Waples, Schindler, Hard, & Kinnison, 2010). However, if the environment
91 keeps on changing, the population might not only deplete its plastic capacity but also
92 its standing genetic variation, which in turn leads to its eventual decline. Further, such
93 a decline would also be conditional on the population's reproductive rate, with higher
94 reproductive rate leading to a slower decline (Juan-Jordá, Mosqueira, Freire, &
95 Dulvy, 2015). In addition, due to continuous changes in the exogenous environment,
96 selection pressures can subsequently increase leading to contemporary evolution
97 (Yoshida, Jones, Ellner, Fussmann, & Hairston, 2003). Adaptive evolution would

then depend on the amount of genetic variation present in the population with higher variation leading to faster evolution, which can either stabilize or destabilize population dynamics (Cortez, 2016; Sanchez & Gore, 2013). Since the dynamics of a population in response to an exogenous pressure is determined by the shape of its potential energy landscape (Beisner et al., 2003), it is thus expected that these factors namely plasticity, genetic variation, and reproductive rate have the capacity to influence the shape of the ball-in-cup landscape. In turn, given that EWS are stability measures derived from alternative stable states theory (Beisner et al., 2003; Clements & Ozgul, 2018; Scheffer et al., 2009a), it is very likely that strength in EWS and hence predictability of population decline might also be affected by these factors. Such theoretical expectations raise important practical questions: can predictability of population decline with the help of EWS be affected by such ecological and evolutionary factors?

Abundance-based measures of the stability of an ecological system might not be the only indicators of a population being forced by an external environment (Clements & Ozgul, 2016b) . Phenotypic traits, such as body size, is one of the important traits that determines the fate of individuals as well as dynamics of population, and thus can provide crucial information regarding the current state of the population (Clements and Ozgul 2016b; Ozgul et al. 2014; Spanbauer et al. 2016). Recently, Clements & Ozgul (2016) showed, using data from experimental microcosms, that including body size information with EWS could significantly improve the predictive accuracy of population declines. Such trait-based signals, have been further shown to be present in the historic collapses of whale populations (Clements et al., 2017). However,

extensive research on the efficacy of such signals in comparison to abundance-based EWS is still in its infancy (Clements & Ozgul, 2018).

Here in this paper, we used a quantitative genetics framework to simulate the dynamics of a population in response to gradual environmental change. We track both the population dynamics and trait distribution until the simulated population declines significantly. We show that this particular model exhibits critical slowing down behavior and hence is expected to show EWS. We then assess whether genetic variation, plasticity in the trait, and net reproductive rate alter the ball-in-cup landscape (stability landscape) and consequently the strength in EWS. In addition, we assess the efficacy of trait-based EWS in comparison with abundance-based EWS and reiterate the ability of trait-based signals in accurately informing population declines.

2. Materials and Methods

2.1 Mathematical model:

We model the joint dynamics of quantitative trait evolution and population size under density dependent regulation via the effects of selection (Chevin, Lande, & Mace, 2010; Chevin & Lande, 2010; Gomulkiewicz & Holt, 1995) . We consider a population that has discrete generations where individuals have fitness that is determined by a single quantitative trait z under stabilizing selection with linear reaction norms (Gavrilets & Scheiner, 1993). Under these assumptions the dynamics of the population and the mean value of the trait can be written as (Lande, 2009) :

$$N_{t+1} = N_t \bar{R}_t = R_0^{\left(1-\frac{N}{K}\right)} \overline{W}, \quad (1)$$

$$\overline{z}_{t+1} = \overline{a}_t + \sigma_a^2 \frac{\partial ln\overline{W}}{\partial \overline{a}} + bu_t. \quad (2)$$

$\overline{R_t}$ is the growth rate of the population at generation *t*, R_0 is the net reproductive rate which is under density dependent selection given by the exponent $\left(1 - \frac{N}{K}\right)$ (Chevin & Lande, 2010). The average fitness of the population is given by the equation $\overline{W}$ which is due to the quantitative trait *z*. $\bar{z}_{t+1}$ is the average value of the trait at generation *t+1*, $\bar{a}_t$ is the mean breeding value or genotypic value of the population at generation *t*, $\frac{\partial ln\overline{W}}{\partial \bar{a}}$ is the gradient of selection on the mean trait $\bar{z}$, σ_a^2 is the additive genetic variance, bu_t quantifies the average plastic response of the trait at time *t* , and *u* is the environmental cue (table 1).

Expanding $\bar{W}$ in equation (1) as follows:

$$\overline{W} = \int W(z,\theta)p(z)dz = \sqrt{\frac{\sigma_w^2}{\sigma_z^2+\sigma_w^2}}\, e^{-(\bar{z}_t-\theta_t)^2/2\left(\sigma_w^2+\sigma_z^2\right)}. \quad (3)$$

The integral in (3) over all trait values in the population gives the average fitness of the population. *p(z)* is the distribution of the trait in the population, σ_z^2 is the variance in the phenotypic distribution *p(z)* and $W(z,\theta)$ is the gaussian stabilizing fitness function given as:

$$W(z) = e^{-(z-\theta)^2/\,2\left(\sigma_w^2\right)}, \quad (4)$$

with width w_z^2 and optimum phenotype of θ. Individuals with trait values far from the optimum will have lower fitness compared to individuals whose trait value matches the optimum phenotype θ. Hence an individual's fitness will be determined by how far its trait value *z* is from the optimum phenotype θ (Chevin and Lande, 2010). Finally, the response of the primary phenotype *z* of an individual in this finite population to the external environment is modeled using linear reaction norms (Gavrilets and Scheiner, 1993; Lande and Shannon, 1996) :

$$z_{i,t} = a_{i,t} + bu_t + \epsilon \quad (5)$$

where a is the breeding value of the individual i. The breeding value is normally distributed with mean $\overline{a}$ and additive genetic variance σ_a^2, and ϵ is the residual component with mean 0 and variance σ_ϵ^2. The slope b quantifies how plastic the trait z is in response to the environment. In our model b is constant meaning that plasticity in the trait cannot evolve (Chevin & Lande, 2010). We model an environment and the environmental cue (see below) that determines the optimal phenotypic value θ_t for the primary phenotype z. The optimal phenotype θ_t, is assumed to be linearly dependent on the external environment E that selects for a particular phenotypic value such that,

$$\theta_t = BE_t. \tag{6}$$

Expanding equation 6, the dynamics of the optimal phenotype is:

$$\theta_t = BE_t = \begin{cases} 0 & , t < 500 \\ B - B\frac{t}{500} & , t \geq 500 \end{cases} \tag{6a}$$

And the environmental cue u in equation (5) is modeled as:

$$u_t = \begin{cases} 0 & , t < 500 \\ c - c\frac{t}{500} & , t \geq 500 \end{cases} \tag{7}$$

Environmental change is modeled at t = 500, where a shift in the external environmental value E_t also triggers a shift in the optimum phenotypic value. The rate of the shift in the optimum phenotypic value is controlled by the parameter B (equation 6a, see section 2.4 below). As in Reed et al. (2010), the dynamics of the optimal phenotype θ in equation (6a) and the environmental cue u in equation (7) are modelled to be correlated over time. This correlation is modeled by taking the help of a bivariate normal distribution: at each generation t, a value for the optimal phenotype θ and environmental cue u are drawn randomly from a bivariate normal distribution with means given by equation (6a) and (7). The covariance of the bivariate normal

190 distribution is given by $\sigma_{\theta,u} = \xi\sigma_\theta\sigma_u$ where ξ is the correlation between θ and the
191 cue *u*. If $\xi = 1$, then the values of the optimum phenotype and the environmental cue
192 drawn from the bivariate normal distribution will be perfectly correlated over time *t*
193 and when $\xi = 0$, they will not be correlated. Thus, ξ determines predictability of the
194 external environment such that ξ = 1 means that an individual is able to perceive
195 changes in the external environmental perfectly with the help of an environmental cue
196 *u* that is correlated with the changes in the external environment. In such a case, the
197 plastic response will track the changes in the environment and the strength of the
198 plastic response of the trait will be determined by *b*. We assumed that variances in the
199 cue σ_u and the optimum σ_θ are equal (see table 1). This mimics the situation, for
200 instance, when variation in food availability is correlated with inter annual variation
201 in snow melt (Vuren & Armitage, 1991) - where in this case, inter annual variation of
202 snow melt is the environmental cue *u* that the organism perceives, and variation in
203 food availability is the external environment *E*. Depending on the changes in the
204 external environment (for example, changes in food availability), the optimum
205 phenotype θ will change which is given by equation 6.

206 The above model is based on the infinitesimal quantitative genetic model (Chevin &
207 Lande, 2010; Falconer & Mackay, 1996).
208
209 *2.2 Stability landscape and effective potential:* One approach to quantifying stability
210 which is also fundamental to dynamical systems with alternative stable states is the
211 'ball-in-cup' analogy (Haydon, 2003; Villa Martín et al., 2015). The different states of
212 the dynamical system can be represented by a landscape and the state of the
213 population at a particular moment by a ball in that landscape. The landscape of the
214 dynamical system can be represented by an effective potential $V(n)$ (Beisner et al.,

2003; Villa Martín et al., 2015). If a dynamical system (example a population) can be represented by a continuous differential equation in the form of: $\frac{dn}{dt} = g(n)$, then the effective potential of that dynamical system can be written as : $V(n) = -\int g(n)dn$ (Beisner et al., 2003; Nolting & Abbott, 2015). For our dynamical system, $g(n) = \log\left(R_0^{\left(1-\frac{n}{k}+\beta-\gamma\right)}\right)$ (see appendix 4). Here *n* is the state of the system, which in our case is the log of the population size *N*. The effective potential of our dynamical system is then (appendix 4):

$$V(n) = -\left(rn - \frac{\frac{r}{k}n^2}{2} + \beta rn - \gamma rn \right)$$

$$= -\left(rn - \frac{\frac{r}{k}n^2}{2} + \frac{\log\left(\frac{\sqrt{(\sigma_w^2)}}{\sqrt{(\sigma_w^2+\sigma_z^2}}\right)}{\log(R_0)}rn - \frac{(\bar{a} + bu_t - \theta)^2}{(R_0(\sigma_w^2+\sigma_z^2))}rn \right) \quad (8)$$

It is evident from the above equation (8) that the effective potential function is dependent on three parameters: r, β, γ, where r = log(R_0); $\beta = \frac{\log\left(\frac{\sqrt{(\sigma_w^2)}}{\sqrt{(\sigma_w^2+\sigma_z^2}}\right)}{\log(R_0)}$; $\gamma = \frac{(\bar{z}-\theta)^2}{(R_0(\sigma_w^2+\sigma_z^2))}$; n = log(N); k= log(K). β represents the standing load of the population and γ represents the lag-load.

2.3 Equilibria and eigenvalues of the model: The extinction equilibrium for the model is at *N* = 0* and the positive equilibrium for the model is at $N^* = K + \beta K - \gamma K$, where γ is the lag-load and β represents the standing load of the population (see appendix 1). Stability of the two equilibria are based on their corresponding eigenvalues, $\lambda = \frac{\partial}{\partial N} f(N)|_{N=N^*}$. Equilibria will be stable if magnitude of $\lambda < 1$ and

unstable if magnitude of $\lambda > 1$. For details of linear stability analysis and occurrence of CSD see appendix 1 and appendix 2.

2.4 Simulations of population declines: We performed stochastic simulations of the model described in section 2.1. Dynamics of the trait, population and the external environment were iteratively updated using equations (1- 7). Without loss of generality, the mean phenotypic value $\bar{z}_0 = \theta = 0$, at the start of the simulation, i.e., at t=0 (equation 6a). This meant that initially before a shift in the external environment, average phenotypic value of the population is at its optimum. External environmental change in our model was enforced at t=500 after the populations had reached the carrying capacity. Stochasticity in the model was introduced at each generation *t* by randomly drawing both optimum phenotypic value and the environmental cue from a bivariate normal distribution with means given by equation 6a and 7 respectively, and covariance given by $\sigma_{\theta,u} = \xi\sigma_\theta\sigma_u$, where σ_θ and σ_u quantifies the variance in the fluctuation of optimum phenotype and the environmental cue over time *t*. Environmental predictability in our model was set at $\xi = 1$, which meant that the external environmental change and the environmental cue drawn at each generation *t* were highly correlated (see Reed et al. 2010). We forced the populations to decline by changing the rate of change in the environment E_t, at t= 500. We chose a rate of change in the environment in a way that populations declined regardless of any combination of parameter values. This was done by setting B =20 in (6a) in all of our simulations, after $t \geq 500$. In all of our simulations, for each parameter value of a factor (genetic variation, plasticity, net reproductive rate) we did 100 independent simulations of population declines.

2.4.1 Abundance-based EWS: For abundance-based EWS analyses, the length of the time-series used was of the same length for each factor (genetic variation, plasticity, net reproductive rate) in question. For each parameter value of each factor in question, we used 30 time-series data after the time point of environmental change i.e., after t= 500 to t=530. We discarded the rest of time-series data. We chose a rate of environmental change in a way (B=20) that population decline was not immediate. Significant population declines were observed across replicates for different factors after t = 530 time point (see timeseries data, Fig. S3-S5). Next, we analyzed 30 abundance data points after t=500, when the environmental change sets in. This ensured normalization of the length of each time series and minimized the effect of varying length of timeseries. We then applied generic EWS of population collapse by using the *earlywarnings* package in R. We focused our analysis on two specific indicators namely autocorrelation at the first-lag (AR1) and standard deviation (SD) as most of the other indicators – such as first-order autoregressive coefficient or coefficient of variation – could be theoretically derived from these parameters (Dakos et al. 2012). These two EWSs are theorized to increase over time before a significant population decline (Dakos, Carpenter, van Nes, & Scheffer, 2014; Scheffer et al., 2009a). Thus, the important question is whether these two EWSs increases before significant population declines that was observed after time point t = 530 (see Fig. S3-5). If the two EWSs increased over time before significant population declines, were their performances affected by the different ecological and evolutionary factors?

The two indicators AR1 and SD were calculated using a predefined sliding window which was 50% of the abundance time-series being analyzed. We z-standardized the leading indicators so that it would be easier to incorporate information from

phenotypic trait later in our analyses. We used Gaussian detrending to remove any trend in the abundance time-series and used Kendall's Tau correlation coefficient of the indicators prior to time point t=530 as an indicator of an approaching decline. Kendall's tau is a non-parametric measure of rank correlation used to identify an increasing trend. Kendall's tau takes values in the range of [-1,1]. Strong positive Kendall's Tau correlations of the statistical indicators (SD and AR1) with time would indicate an approaching population decline (Dakos et al. 2012). If Kendall's tau correlation coefficient for an EWS was less than 0.5, we considered that EWS as a false negative. Hence, we quantified reliability of EWS as the rate of false negatives: the number of times in replicate simulations the Kendall's tau correlation coefficient was less than 0.50. Higher proportion of false negatives would indicate less reliability of EWS and vice-versa.

2.4.2 Trait-based EWS: To evaluate the efficacy of trait-based EWS (Clements & Ozgul, 2016b), information from mean phenotype $\bar{z}$ was incorporated with the leading indicators in an additive manner (Clements *et al.*, 2017; Clements and Ozgul, 2018). To include information from average phenotypic value, we first z-standardized the trait time-series. The length of the phenotypic time-series that was used was the same as the corresponding abundance time-series. Before a population decline, SD and AR1 are expected to increase over time, while in our model, because of the direction of the optimum environmental change, the trait is expected to decline (it is also possible for trait to increase over time, but that would depend on the direction of the optimum phenotypic change). Such a phenotypic trait, for example, could be body size. Body size is a quantitative trait fundamental to life-history theory and population dynamics (Cameron, O'Sullivan, Reynolds, Piertney, & Benton, 2013; Gibert, Allen, Hruska, & DeLong, 2017; Pigeon, Ezard, Festa-Bianchet, Coltman, & Pelletier,

2017), which has been shown to decline in response to decreases in resource availability (Clements & Ozgul, 2016b), increases in temperature (Forster, Hirst, & Atkinson, 2011, 2012; Gardner, Peters, Kearney, Joseph, & Heinsohn, 2011; Tseng et al., 2018), and increases in harvest rate (Frank *et al.*, 2011; Clements *et al.*, 2017). Whether including trait information improves predictability of population decline will be dependent on whether the trait responds to an external environmental change. Here, in our model, the optimum environmental change will affect the dynamics of the phenotype. However, whether the change in the dynamics of the phenotype will occur within the time series length being analyzed here and hence be informative of population decline is unknown. It has been shown that it is possible for shifts in phenotypic dynamics to precede population declines, but only under certain environmental circumstances (Baruah *et al.*, 2018 *(in press)*). As of yet, extensive analysis of the efficacy of EWS and trait-based EWSs has not been done.

Since the phenotype is expected to decrease in response to the change in the optimum environment, the z-standardized values of phenotypic timeseries were multiplied by -1 so that they could be included with the other two standardized statistical metrics such as SD and AR1. The values of standardized EWS such as SD and AR1 were added additively with standardized mean phenotypic time series to quantitatively create trait-based signals or trait-based EWS. We evaluated three trait-based EWS metrics namely *AR1+trait, AR1+SD+trait, SD+trait* and compared how the metrics that included information from the mean phenotype improved predictability of population declines when compared with the abundance-based EWS like *AR1, SD.* We quantified Kendall's Tau correlation coefficient as an indicator for strength of predictability of population declines and reliability of the trait-based EWS as the rate of false negatives.

2.4.3 Adaptive plasticity: To assess the role of adaptive plasticity *b*, we simulated 100 replicate population declines for each parameter value of *b*, which ranged from low to high: 0.05, 0.1, 0.3, 0.4, and 0.8. While we varied plasticity, we fixed $\sigma_a^2 = 0.25$, and R_0 at 1.2. The width of the fitness function determines the strength of selection in the trait. We fixed the width of the fitness function at $\sigma_w^2 = 20$, which would indicate medium strength in selection. Usually, $\sigma_w^2 = 50$ would indicate weak strength in selection and $\sigma_w^2 = 5$ would indicate strong selection (Chevin and Lande 2010).

2.4.4 Genetic variation: The levels of genetic variation σ_a^2 used for the simulations of population declines are 0.05, 0.1, 0.2, 0.3, 0.4, 0.5. Adaptive plasticity *b*, net reproductive rate R_0 and σ_w^2 were kept at 0.2, 1.2 and 20 respectively.

We also did simulations where we relaxed the assumption of genetic variation (σ_a^2) remaining constant during population collapses. For details see appendix 5.

2.4.5 Net reproductive rate: To assess the role R_0, we simulated 100 replicate population declines. The levels of R_0 used for the simulations of population collapse were 1.1, 1.2, 1.3, 1.4, and 1.5. Adaptive plasticity *b*, genetic variation σ_a^2 and σ_w^2, were kept at 0.2, 0.25 and 20 respectively.

3. Results

3.1 Effective potential

3.1.1 Strength of plasticity : The term $\gamma = \frac{(\bar{z}-\theta)^2}{(R_0(\sigma_w^2+\sigma_z^2))}$ in equation (8) is the evolutionary lag due to maladaptation of the mean phenotype with the optimum (Lande, 2009). The effective potential becomes narrower with increasing strength of plasticity and consequentially increases stability, i.e., the potential function becomes more negative (Fig. 2). Since return time and stability are inversely related (Dai et al., 2015), return time decreases with increasing strength of plasticity (Appendix 2, Fig.

S1). In other words, the population quickly recovers with every perturbation if strength of plasticity is high.

3.1.2 Genetic variation: The mean phenotype has variance of $\sigma_z^2 = \sigma_a^2 + \sigma_\epsilon$. Assuming residual component σ_ϵ to be zero, phenotypic variance is then equal to additive genetic variance, $\sigma_z^2 = \sigma_a^2$. Inspection of the equation (8) reveals that high additive genetic variance causes the effective potential to be more positive when compared with low σ_a^2 and consequently decreases stability, i.e., the effective potential becomes less negative (Fig. 2; the more negative the effective potential, more stable the population is). Reduction of stability and effective potential energy is higher for populations with low genetic variance whenever they are forced to collapse compared to populations with high genetic variance (Fig. 2). Further, return time also increases with increasing additive genetic variance (Appendix 2, Fig. S1).

3.1.3 Net reproductive rate: From equation (8), we also see that higher values of R_0 lead to higher stability and narrow potential curve for a given state of the population (Fig. 2). Loss in stability is more when R_0 is higher for the same rate of change in the environmental change when compared with a lower R_0. Further, return time also decreases with increasing R_0 (appendix 2, Fig. S1).

3.2 Simulations of population declines: abundance-based EWS

3.2.1 Strength of plasticity: The strength of EWSs of population collapse (Kendall's Tau value) was much higher in populations which had high adaptive plasticity $\boldsymbol{b}$ = 0.8 (Fig. 3A, B) when compared with populations with low adaptive plasticity. Moreover, the rate of false negatives decreased for all the abundance and trait-based metrics as strength of plasticity increased (Fig. 5A). Rate of false negatives however remained more or less same for AR1 across different plasticity levels (Fig. 5A).

3.2.2 Genetic variation: Higher genetic variation in the population led to slight decrease in detectability of population decline than in populations with lower genetic variation, particularly for SD (Fig. 3C, D). Moreover, the rate of false negatives for SD, AR1 remained more or less same as genetic variation decreased (Fig. 5B). For trait-based EWSs, particularly for *SD+trait*, rate of false negatives was the lowest (Fig. 5B).

3.2.3 Net reproductive rate: Strength in EWS was lower in populations with lower R_0 when compared with higher R_0, particularly for SD (Fig. 3E). AR1 however showed a slightly different result (Fig. 3F). In case of reliability of abundance-based EWS, the rate of false negatives decreased for SD as net reproductive rate increased (Fig. 5C). However, for AR1 rate of false negatives remained unchanged as R_0 increased (Fig. 5C).

3.3 Simulations of population declines: trait-based EWS: Trait-based EWS improved the strength of EWS of population declines (Fig. 4, Fig S8-S9). In principle, *AR1* was the least efficient of all the signals compared. However, when trait information was included with *AR1*, strength in trait-based *AR1 (trait+AR1)* improved significantly (Fig.4, Fig. 5). Overall, the Kendall's Tau value of SD and *SD+trait* was relatively higher than all the other trait-based and abundance-based EWS. This was consistent across all the factors analyzed such as genetic variation, plasticity (Fig.4, Fig. S8-S9). The rate of false negatives was highest for AR1 across all factors analyzed (Fig. 5A-C). For plasticity, the rate of false negatives decreased as strength of plasticity increased, but this was however opposite for genetic variation where the false negatives slightly increased as genetic variance increased (Fig. 5B). Furthermore,

403 even though AR1 had the highest number of false negatives, false negatives of
404 *AR1+trait* significantly decreased (Fig. 5).

405 **4. Discussion**

406 The early detection of population declines with the help of EWS provides a unique
407 tool to highlight conservation efforts to a population approaching an impending
408 transition. We show in this paper that factors intrinsic to a population in question such
409 as genetic variation, plasticity or net reproductive rate could significantly alter
410 stability of a population as well as strength and reliability of EWS of population
411 decline.

412 The detectability of EWSs is dependent not only on the relation between stability and
413 resilience but is also determined by a variety of factors including sampling frequency,
414 and the strength and type of external forcing (Dai, Korolev, and Gore 2015; Clements
415 et al. 2015a; Clements and Ozgul 2016). Here we add to this body of knowledge by
416 demonstrating that the stability of a system can also be altered by intrinsic factors
417 such as genetic variation, plasticity and net reproductive rate. These changes to the
418 effective potential in turn led to stronger EWS being observed, whenever changes in
419 the external optimum caused a population to lose a significant amount of effective
420 potential energy (Fig. 1). In other words, stronger EWSs would be observed whenever
421 a population is forced to move from a deeper point in the potential energy curve
422 (more stable) to its tipping point compared to another population, which is lying on a
423 shallower potential (less stable) (Fig. 2). Our findings also suggested that the utility of
424 EWS was strongly determined by factors that are intrinsic to a population such as
425 genetic variation, net reproductive rate and plasticity.

Higher strength of plasticity in the phenotype significantly affected the detectability of population collapse (Fig. 2). Strength of plasticity altered the response and the dynamics of a population to changes in the external environment. When plasticity was high the response of the phenotype tracked the environment perfectly causing the population to stabilize in response to fluctuating changes in the environment (Fig. S3) (Charmantier et al., 2008; Reed, Schindler, & Waples, 2011). The stability of a population is also reflected in short return time to equilibrium (van Nes & Scheffer, 2007). This was true for the case where the strength of plasticity was high (Fig. S1). Moreover, the basin of attraction for a highly plastic population was deeper when compared to a less plastic population, which was shallower. To push a highly plastic population from the deepest point in its effective potential energy curve to the tipping point, the energy loss would be more, compared to a less plastic population which was lying in a much shallower basin. The loss in energy from driving the highly plastic population from the deepest point to its tipping point was reflected in stronger EWS when one compared it with another less plastic population. Consequently, for the same rate of change in the environment, higher values of plasticity lead to stronger and more reliable EWS of population collapse.

Similarly, the effective potential of our dynamical system was also altered by genetic variation (Fig. 2), with higher genetic variation leading to a shallower stability landscape than that of a population with lower genetic variation. High additive genetic variance created what was called a 'genetic load' that lowered the overall population growth rate (Lande 1976; Lande and Shannon 1996; Chevin, Lande, and Mace 2010). This was due to stabilizing selection acting on the mean phenotype. Due to this genetic load caused by high additive genetic variance, population growth rate at equilibrium was lower causing the effective potential to be closer towards the tipping

point compared to another population having a lower genetic variation. Hence for the same rate of external environmental change, the loss of potential energy was different when one compared a population with high genetic variation to that with low genetic variation. As a result, the performance of EWS was affected with slightly lower detectability and lower reliability of population collapse when there was higher genetic variation (Fig. 3, Fig. 5B). This result however did not mean that genetic variation was detrimental for long-term population persistence. Time to extinction was however longer for populations with higher genetic variation when compared with a population which had a lower genetic variation in the trait (Fig S2)(Robinson, Wares, & Drake, 2013; Willi & Hoffmann, 2009). High genetic variation is necessary for rapid adaptation via genetic evolution, which then aids in evolutionary rescue (Ashander, Chevin and Baskett, 2016). However, our model simulations and analyses of EWS were mainly focused on short transient dynamics after the start of the external optimum change. Further, due to continuous and fast rate of environmental deterioration, adaptation or evolutionary rescue by genetic evolution (Lande 2009; Chevin and Lande 2010) was not possible in our model and the populations eventually declined.

Decreasing population size in response to environmental deterioration and directional selection acting towards a mean phenotype could both lead to depletion of additive genetic variance (Barton & Keightley, 2002). We took this account in our simulations by following a framework developed in (Bu□rger, 2000) (see appendix 5). Using this framework, we find that depletion of genetic variation over time did not affect the strength of EWS compared with when genetic variation remained constant (See Fig S6).

475 Net reproductive rate also had a significant effect on the stability of populations,
476 detectability and reliability of EWS of population collapse. Higher net reproductive
477 rate buffered the population from declining immediately after the environment shifted
478 when compared to a population with lower reproductive rate (Juan-Jordá et al., 2015).
479 Consequently, for the same rate of change in the external optimum environment,
480 populations with lower reproductive rate recovered slowly due to a wide basin of
481 attraction than populations with higher net reproductive rate (Fig. 2, Fig. S1) and
482 hence strength in EWS was more pronounced in the latter.

483 Our modeling results suggested that including fitness-related trait information could
484 significantly improve the strength and reliability in EWS of population collapse.
485 Trait-based EWS (*SD+trait*) produced strongest and reliable signals. Inclusion of
486 phenotypic trait information alongside the leading indicators produced less
487 distributed, consistent and stronger Kendall's tau values compared to the generic
488 abundance-based EWS (Fig. 4, Fig S7-S8). This is because in response to a
489 directional change in the external optimum environment, shift in the mean phenotypic
490 trait occurred over time even if there were no significant increases in either AR1 or
491 SD. Furthermore, including information from the mean phenotype alongside EWS
492 statistics would depend not only on whether the mean phenotype responded to the
493 external forcing but also on the nature of the external environmental forcing itself
494 (Clements & Ozgul, 2016b). Body size is suggested to be an ideal candidate to be
495 included with the leading indicators (Clements & Ozgul, 2016b). Shifts in body size
496 have previously been shown to occur before population collapse in whales, with true
497 positive EWS being detectable earlier when information from the body size was
498 included in the EWS (Clements et al., 2017). Furthermore, it has been suggested that

499 in certain environmental change scenarios, it is possible for body size to shift before a
500 population decline and thus act as a warning signal (Baruah *et al.*, 2018 *(in press)*).

501 In conclusion, we showed that predictability of population decline was affected by
502 factors intrinsic to a population like genetic variation, strength in adaptive plasticity
503 and net reproductive rate. Changes in these factors can not only alter the underlying
504 phenotypic and population dynamics, but also the effective potential landscape.
505 Consequently, due to the alteration of the effective potential landscape, the
506 detectability of EWS was hampered. However, if information from fitness-related
507 trait was incorporated with EWS, the strength in predicting population collapses
508 increased significantly. Our results suggests that the inclusion of trait dynamic
509 information alongside the generic EWS should provide more accurate forecasts of the
510 future state of biological systems.

511 **5. Code availability**: R version 3.5.1. R script for the code is made available:
512 https://github.com/GauravKBaruah/Eco-Evo-EWS

513 **6. Data availability:** will be made available at Dryad repository.

514 **7. Author contributions:**

515 GB conceived the ideas and designed the methodology; GB analyzed the data with
516 feedback from CFC and AO; All authors contributed to the drafts and final approval
517 for submission.

518 **8. References**

519 Ashander, J., Chevin, L.-M., & Baskett, M. L. (2016). Predicting evolutionary rescue
520 via evolving plasticity in stochastic environments. *Proceedings of the Royal*

Society B: Biological Sciences, *283*(1839), 20161690. doi:10.1098/rspb.2016.1690

Barton, N. H., & Keightley, P. D. (2002). Understanding quantitative genetic variation. *Nature Reviews. Genetics*, *3*(1), 11–21. doi:10.1038/nrg700

Baruah, G., Clements, C. F., Guillaume, F., & Ozgul, A. (2018). When do shifts in trait dynamics precede population declines? *BioRxiv*, 424671. doi:10.1101/424671

Beisner, B., Haydon, D., & Cuddington, K. (2003). Alternative stable states in ecology. *Frontiers in Ecology and the Environment*, *1*(7), 376–382. doi:10.1890/1540-9295(2003)001[0376:ASSIE]2.0.CO;2

Boettiger, C., & Hastings, a. (2012a). Early warning signals and the prosecutor's fallacy. *Proceedings of the Royal Society B: Biological Sciences*, *279*(1748), 4734–4739.

Boettiger, & Hastings. (2012b). Quantifying limits to detection of early warning for critical transitions. *Journal of The Royal Society Interface*. doi:10.1098/rsif.2012.0125

Bu□rger, R. (Reinhard). (2000). *The mathematical theory of selection, recombination, and mutation*. Wiley.

Butitta, V. L., Carpenter, S. R., Loken, L. C., Pace, M. L., & Stanley, E. H. (2017). Spatial early warning signals in a lake manipulation. *Ecosphere*, *8*(10), e01941. doi:10.1002/ecs2.1941

Cameron, T. C., O'Sullivan, D., Reynolds, A., Piertney, S. B., & Benton, T. G.

(2013). Eco-evolutionary dynamics in response to selection on life-history. *Ecology Letters*, *16*(6), 754–63. doi:10.1111/ele.12107

Cardillo, M., Mace, G. M., Jones, K. E., Bielby, J., Bininda-Emonds, O. R. P., Sechrest, W., … Purvis, A. (2005). Multiple causes of high extinction risk in large mammal species. *Science (New York, N.Y.)*, *309*(5738), 1239–41. doi:10.1126/science.1116030

Charmantier, A., McCleery, R. H., Cole, L. R., Perrins, C., Kruuk, L. E. B., & Sheldon, B. C. (2008). Adaptive phenotypic plasticity in response to climate change in a wild bird population. *Science (New York, N.Y.)*, *320*(5877), 800–803. doi:10.1126/science.1157174

Chevalier, M., & Grenouillet, G. (2018). Global assessment of early warning signs that temperature could undergo regime shifts. *Scientific Reports*, *8*(1), 10058. doi:10.1038/s41598-018-28386-x

Chevin, L. M., Lande, R., & Mace, G. M. (2010). Adaptation, plasticity and extintion in a changing enviroment: towards a predictive theory. *PLoS Biology*, *8*(4), 1–8.

Chevin, & Lande. (2010). When do adaptive plasticity and genetic evolution prevent extinction of a density-regulated population? *Evolution*, *64*(4), 1143–1150. doi:10.1111/j.1558-5646.2009.00875.x

Clements, Blanchard, J. L., Nash, K. L., Hindell, M. A., & Ozgul, A. (2017). Body size shifts and early warning signals precede the historic collapse of whale stocks. *Nature Ecology & Evolution*, *1*(7), 0188. doi:10.1038/s41559-017-0188

Clements, C. F., & Ozgul, A. (2016a). Rate of forcing and the forecastability of

565 critical transitions. *Ecology and Evolution, In press*(April), 7787–7793.
566 doi:10.1002/ece3.2531

567 Clements, Drake, J. M., Jason, I. G., & Ozgul, A. (2015). Factors Influencing the
568 Detectability of Early Warning Signals of Population Collapse. *The American*
569 *Naturalist*, *186*(1), 50–58. doi:10.1086/681573

570 Clements, & Ozgul, A. (2016b). Including trait-based early warning signals helps
571 predict population collapse. *Nature Communications*, *7*, 10984. Retrieved from
572 http://www.nature.com/doifinder/10.1038/ncomms10984

573 Clements, & Ozgul, A. (2018). Indicators of transitions in biological systems.
574 *Ecology Letters*, *21*(6), 905–919. doi:10.1111/ele.12948

575 Cortez, M. H. (2016). How the Magnitude of Prey Genetic Variation Alters Predator-
576 Prey Eco-Evolutionary Dynamics. *The American Naturalist*, *188*(3), 329–41.
577 doi:10.1086/687393

578 Dai, L., Korolev, K. S., & Gore, J. (2013). Slower recovery in space before collapse
579 of connected populations. *Nature*, *496*(7445), 355–358. doi:10.1038/nature12071

580 Dai, L., Korolev, K. S., & Gore, J. (2015). Relation between stability and resilience
581 determines the performance of early warning signals under different
582 environmental drivers. *Proceedings of the National Academy of Sciences of the*
583 *United States of America*, *112*(32), 10056–61. doi:10.1073/pnas.1418415112

584 Dakos, V., Carpenter, S. R., Brock, W. A., Ellison, A. M., Guttal, V., Ives, A. R., …
585 Scheffer, M. (2012). Methods for detecting early warnings of critical transitions
586 in time series illustrated using simulated ecological data. *PLoS ONE*, *7*(7).

587 doi:10.1371/journal.pone.0041010

588 Dakos, V., Carpenter, S. R., van Nes, E. H., & Scheffer, M. (2014). Resilience
589 indicators: prospects and limitations for early warnings of regime shifts.
590 *Philosophical Transactions of the Royal Society B: Biological Sciences*,
591 *370*(1659), 20130263–20130263. doi:10.1098/rstb.2013.0263

592 Dakos, V., Scheffer, M., van Nes, E. H., Brovkin, V., Petoukhov, V., & Held, H.
593 (2008). Slowing down as an early warning signal for abrupt climate change.
594 *Proceedings of the National Academy of Sciences of the United States of*
595 *America*, *105*(38), 14308–12. doi:10.1073/pnas.0802430105

596 Drake, J. M., & Griffen, B. D. (2010). Early warning signals of extinction in
597 deteriorating environments. *Nature*, *467*(7314), 456–9. doi:10.1038/nature09389

598 Falconer, D. S., & Mackay, T. F. C. (1996). *Introduction to Quantitative Genetics*
599 *(4th Edition)*. *Trends in Genetics* (Vol. 12). Retrieved from
600 http://www.amazon.com/Introduction-Quantitative-Genetics-Douglas-
601 Falconer/dp/0582243025

602 Forster, J., Hirst, A. G., & Atkinson, D. (2011). How do organisms change size with
603 changing temperature? The importance of reproductive method and ontogenetic
604 timing. *Functional Ecology*, *25*(5), 1024–1031. doi:10.1111/j.1365-
605 2435.2011.01852.x

606 Forster, J., Hirst, A. G., & Atkinson, D. (2012). Warming-induced reductions in body
607 size are greater in aquatic than terrestrial species. *Proceedings of the National*
608 *Academy of Sciences of the United States of America*, *109*(47), 19310–4.
609 doi:10.1073/pnas.1210460109

610 Frank, K. T., Petrie, B., Fisher, J. A., & Leggett, W. C. (2011). Transient dynamics of
611 an altered large marine ecosystem. *Nature*. doi:10.1038/nature10285

612 Gardner, J. L., Peters, A., Kearney, M. R., Joseph, L., & Heinsohn, R. (2011).
613 Declining body size: A third universal response to warming? *Trends in Ecology*
614 *and Evolution*. doi:10.1016/j.tree.2011.03.005

615 Gavrilets, S., & Scheiner, S. M. (1993). The genetics of phenotypic of reaction norm
616 shape V . Evolution. *Journal of Evolutionary Biology*, *6*(1), 31–48.
617 doi:10.1046/j.1420-9101.1993.6010031.x

618 Gibert, J. P., Allen, R. L., Hruska, R. J., & DeLong, J. P. (2017). The ecological
619 consequences of environmentally induced phenotypic changes. *Ecology Letters*,
620 *20*(8), 997–1003. doi:10.1111/ele.12797

621 Gomulkiewicz, R., & Holt, R. D. (1995). When does evolution by natural selection
622 prevent extinction? *Evolution*, *49*(1), 201–207. Retrieved from
623 http://www.jstor.org/stable/10.2307/2410305%5Cnpapers2://publication/uuid/A
624 F75FB13-CA45-471F-9595-604002DDAB20

625 Haydon, D. (2003). Alternative stable states in ecology. *Frontiers in Ecology*.
626 doi:10.1890/1540-9295(2003)001[0376:ASSIE]2.0.CO;2

627 Holling, C. S. (1973). Resilience and Stability of Ecological Systems. *Annual Review*
628 *of Ecology and Systematics*, *4*(1), 1–23.
629 doi:10.1146/annurev.es.04.110173.000245

630 Jarvis, L., McCann, K., Tunney, T., Gellner, G., & Fryxell, J. M. (2016). Early
631 warning signals detect critical impacts of experimental warming. *Ecology and*

Evolution. doi:10.1002/ece3.2339

Juan-Jordá, M. J., Mosqueira, I., Freire, J., & Dulvy, N. K. (2015). Population declines of tuna and relatives depend on their speed of life. *Proceedings of the Royal Society B: Biological Sciences*, *282*(1811), 20150322. doi:10.1098/rspb.2015.0322

Krko ek, M., & Drake, J. M. (2014). On signals of phase transitions in salmon population dynamics. *Proceedings of the Royal Society B: Biological Sciences*, *281*(1784), 20133221–20133221. doi:10.1098/rspb.2013.3221

Lande. (2009). Adaptation to an extraordinary environment by evolution of phenotypic plasticity and genetic assimilation. *Journal of Evolutionary Biology*, *22*(7), 1435–1446. doi:10.1111/j.1420-9101.2009.01754.x

Lande, R. (1976). NATURAL SELECTION AND RANDOM GENETIC DRIFT IN PHENOTYPIC EVOLUTION. *Evolution*, *30*(2), 314–334. doi:10.1111/j.1558-5646.1976.tb00911.x

Lande, & Shannon. (1996). THE ROLE OF GENETIC VARIATION IN ADAPTATION AND POPULATION PERSISTENCE IN A CHANGING ENVIRONMENT. *Evolution*, *50*(1), 434–437. doi:10.1111/j.1558-5646.1996.tb04504.x

Nolting, B. C., & Abbott, K. C. (2015). Balls, cups, and quasi-potentials: quantifying stability in stochastic systems. *Ecology*, *97*(4), 15–1047.1. doi:10.1890/15-1047.1

Ozgul, A., Bateman, A. W., English, S., Coulson, T., & Clutton-Brock, T. H. (2014).

Linking body mass and group dynamics in an obligate cooperative breeder. *Journal of Animal Ecology*, *83*(6), 1357–1366. doi:10.1111/1365-2656.12239

Ozgul, A., Childs, D. Z., Oli, M. K., Armitage, K. B., Blumstein, D. T., Olson, L. E., … Coulson, T. (2010). Coupled dynamics of body mass and population growth in response to environmental change. *Nature*, *466*(7305), 482–485. Retrieved from http://dx.doi.org/10.1038/nature09210

Pigeon, G., Ezard, T. H. G., Festa-Bianchet, M., Coltman, D. W., & Pelletier, F. (2017). Fluctuating effects of genetic and plastic changes in body mass on population dynamics in a large herbivore. *Ecology*, *98*(9), 2456–2467. doi:10.1002/ecy.1940

Price, T. D., Qvarnström, A., & Irwin, D. E. (2003). The role of phenotypic plasticity in driving genetic evolution. *Proceedings of the Royal Society - Biological Sciences*. doi:10.1098/rspb.2003.2372

Reed, T. E., Schindler, D. E., & Waples, R. S. (2011). Efectos Interactivos de la Plasticidad Fenot??pica y Evoluc??on sobre la Persistencia Poblacional en un Clima Cambiante. *Conservation Biology*, *25*(1), 56–63. doi:10.1111/j.1523-1739.2010.01552.x

Reed, T. E., Waples, R. S., Schindler, D. E., Hard, J. J., & Kinnison, M. T. (2010). Phenotypic plasticity and population viability: the importance of environmental predictability. *Proceedings. Biological Sciences / The Royal Society*, *277*(1699), 3391–400. doi:10.1098/rspb.2010.0771

Robinson, J. D., Wares, J. P., & Drake, J. M. (2013). Extinction hazards in experimental Daphnia magna populations: Effects of genotype diversity and

677 environmental variation. *Ecology and Evolution*. doi:10.1002/ece3.449

678 Sanchez, A., & Gore, J. (2013). Feedback between Population and Evolutionary
679 Dynamics Determines the Fate of Social Microbial Populations. *PLoS Biology*,
680 *11*(4), e1001547. doi:10.1371/journal.pbio.1001547

681 Scheffer, Bascompte, Brock, W. A., Brovkin, V., Carpenter, S. R., Dakos, V., …
682 Sugihara, G. (2009a). Early-warning signals for critical transitions. *Nature*, *461*,
683 53–59. Retrieved from http://dx.doi.org/10.1038/nature08227%5Cn%3CGo to
684 ISI%3E://WOS:000269478800026%5Cnhttp://www.nature.com/nature/journal/v
685 461/n7260/pdf/nature08227.pdf

686 Scheffer, M., Bascompte, J., Brock, W. A., Brovkin, V., Carpenter, S. R., Dakos, V.,
687 … Sugihara, G. (2009b). Early-warning signals for critical transitions. *Nature*,
688 *461*(7260), 53–59. doi:10.1038/nature08227

689 Spanbauer, T. L., Allen, C. R., Angeler, D. G., Eason, T., Fritz, S. C., Garmestani, A.
690 S., … Sundstrom, S. M. (2016). Body size distributions signal a regime shift in a
691 lake ecosystem. *Proceedings of the Royal Society B*, *283*, 20160249.
692 doi:http://dx.doi.org/10.1098/rspb.2016.0249

693 Strogatz, S. H. (1994). Nonlinear Dynamics and Chaos. *Book*, 1–505.
694 doi:9780738204536

695 Thomas, C. D., Thomas, C. D., Cameron, A., Cameron, A., Green, R. E., Green, R.
696 E., … Williams, S. E. (2004). Extinction risk from climate change. *Nature*,
697 *427*(6970), 145–8. doi:10.1038/nature02121

698 Tseng, M., Kaur, K. M., Soleimani Pari, S., Sarai, K., Chan, D., Yao, C. H., …

699 Fograscher, K. (2018). Decreases in beetle body size linked to climate change
700 and warming temperatures. *Journal of Animal Ecology*, *87*(3), 647–659.
701 doi:10.1111/1365-2656.12789

702 van Nes, E. H., & Scheffer, M. (2007). Slow recovery from perturbations as a generic
703 indicator of a nearby catastrophic shift. *The American Naturalist*, *169*(6), 738–
704 747. doi:10.1086/516845

705 Villa Martín, P., Bonachela, J. A., Levin, S. A., & Muñoz, M. A. (2015). Eluding
706 catastrophic shifts. *Proceedings of the National Academy of Sciences*.
707 doi:10.1073/pnas.1414708112

708 Vuren, D. Van, & Armitage, K. B. (1991). Duration of snow cover and its influence
709 on life-history variation in yellow-bellied marmots. *Canadian Journal of*
710 *Zoology*, *69*(7), 1755–1758. doi:10.1139/z91-244

711 Willi, Y., & Hoffmann, A. A. (2009). Demographic factors and genetic variation
712 influence population persistence under environmental change. *Journal of*
713 *Evolutionary Biology*, *22*(1), 124–133. doi:10.1111/J.1420-9101.2008.01631.X

714 Wissel, C. (1984). A universal law of the characteristic return time near thresholds.
715 *Oecologia*, *65*(1), 101–107. doi:10.1007/BF00384470

716 Yoshida, T., Jones, L. E., Ellner, S. P., Fussmann, G. F., & Hairston, N. G. (2003).
717 Rapid evolution drives ecological dynamics in a predator–prey system. *Nature*.
718 doi:10.1038/nature01767

719 **Table 1:** List of parameter values and variables used in the model simulations. The
720 variables are not given any value but factors for which the model simulations are

721 tested are given values.

Parameters/variables	Description	Value
N_t	Abundance of the population at time t	....
$\bar{z}_t$; $\bar{a}_t$	Mean trait value at time t; mean breeding value at time t	....
σ_z^2; σ_a^2	Variance of the mean trait; additive genetic variance or variance of the mean breeding value	[0.05, 0.1, 0.2, 0.3, 0.4,0.5] ; [0.05,0.1, 0.2, 0.3, 0.4,0.5]
b	Strength in phenotypic plasticity	[0.05, 0.1, 0.3,0.4, 0.8]
R_0	Net reproductive rate	[1.1, 1.2,1.3,1.4, 1.5]
u_t	Environmental cue at time *t*	$U_t = \begin{cases} 0 & , t < 500 \\ 1 - c\frac{t}{500} & , t \geq 500 \end{cases}$
θ_t	Optimum phenotype at time *t*	$\theta_t = BE_t = \begin{cases} 0 & , t < 500 \\ B - B\frac{t}{500} & , t \geq 500 \end{cases}$ (B = 20)
w_z^2	Width of the Gaussian stabilizing fitness function. A measure of the strength in selection	20
z_i, a_i	Trait value for an individual *i* ; breeding value for an individual *i*	....
ϵ	Residual component or unexplained component of a trait z	0
σ_ϵ^2	Variance in that residual component ϵ	0
E_t	External environmental value at time *t*	….
B	Coefficient that captures the strength in the external environmental change	20
c	Coefficient that controls the rate of change in the environmental cue	5
ξ	Environmental predictability;	1

	quantifies how much the external environment is correlated with the environmental cue	
σ_θ, σ_u	Variance in optimum phenotype, variance in environmental cue	1.25^2, 1.25^2

722

723

724

725 *Figure Captions:*

726 **Figure 1.** Illustration of the 'ball-in-cup' potential energy curve in relation to
727 stability and resilience of a one-dimensional dynamical system. The stable state of
728 the dynamical system (A) which is an isolated population, can be indicated by the
729 blue ball, and the unstable state (or the tipping point) can be indicated by the red ball
730 in both A and B. (1)- shows that the slope of the potential curve (i.e., stability) is steep
731 and the basin where the ball lies is also wide signifying that both resilience as well as
732 stability is high. This means that the amount of effective potential energy needed (2)
733 to push the ball from its stable state (blue) to the unstable state (red) (or in other
734 words the reduction in stability) will be large. However, for another isolated
735 population, there might be intrinsic differences in ecological or evolutionary factors
736 controlling the dynamics of that isolated population and this might cause (3) a shift in
737 the 'ball-in-cup' potential energy curve from (6) to (4), for that population. In (4) the
738 slope is now less steep, signifying a reduction in intrinsic stability. Along with this,
739 there is also a reduction in intrinsic resilience. Now, the amount of energy (5) to move

740 the blue ball at (4) to the unstable state for (B) is less. This could reflect in the
741 performances of EWS of population declines.
742
743 **Figure 2.** Effective potential $V(N)$ plotted as a function of the state variable
744 abundance, N. Note the effective potential is altered by factors like genetic variation,
745 adaptive plasticity and net reproductive rate. The lower the value of the effective
746 potential, more stable the system is.

747 **Figure 3.** Box plots showing the distribution of Kendall's Tau correlation coefficient
748 (high values around 0.5 are usually considered an EWS) for 100 simulation of
749 population declines for different levels of adaptive plasticity *b*, genetic variation σ_a^2,
750 reproductive rate R_0. The leading indicators that are shown here are autocorrelation at
751 lag-1 (AR1) and standard deviation (SD). X-axis is the different levels of the above
752 factors.

753 **Figure 4.** Box plots showing the distribution of Kendall's Tau correlation coefficient
754 for 100 simulation of population declines for different levels of adaptive plasticity *b*.
755 On the X-axis are the different early warning metrics shown: autocorrelation at lag-1
756 (AR1), standard deviation (SD), *(AR1+SD)*, (*AR1+Tr), (SD+Tr*) ,*(AR1+SD+Tr). Tr*
757 corresponds to the mean value of the phenotypic trait. Colored boxplots denote the
758 trait-based EWS while white boxplots denote abundance-based EWS.

759 **Figure 5.** Proportion of false negatives shown here for a threshold of 0.5 (which
760 means Kendall's tau value below 0.5 are considered not an EWS) on the Y-axis for
761 abundance and trait-based EWS metrics for different levels of (A) plasticity strength ,
762 (B) genetic variation, (C) net reproductive rate.
763

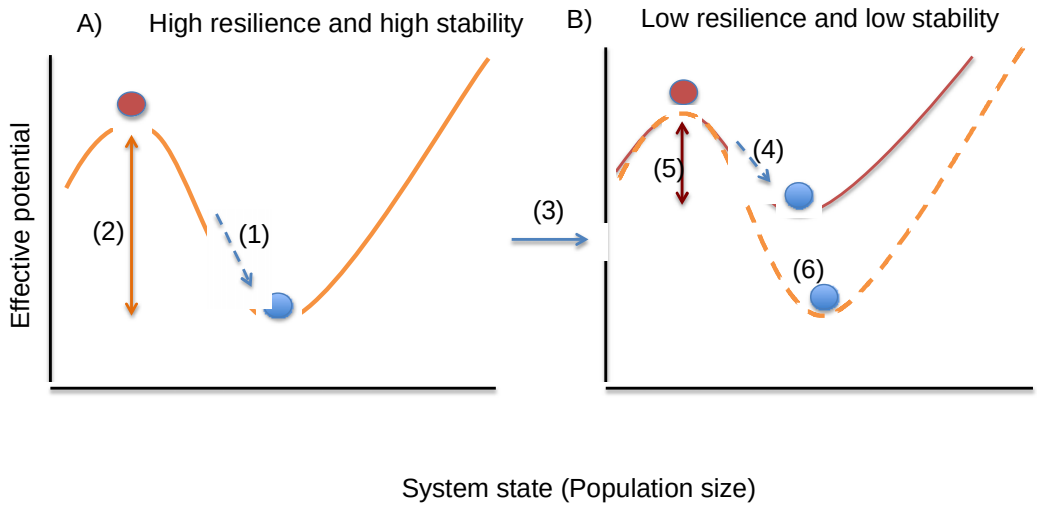

Figure 1.

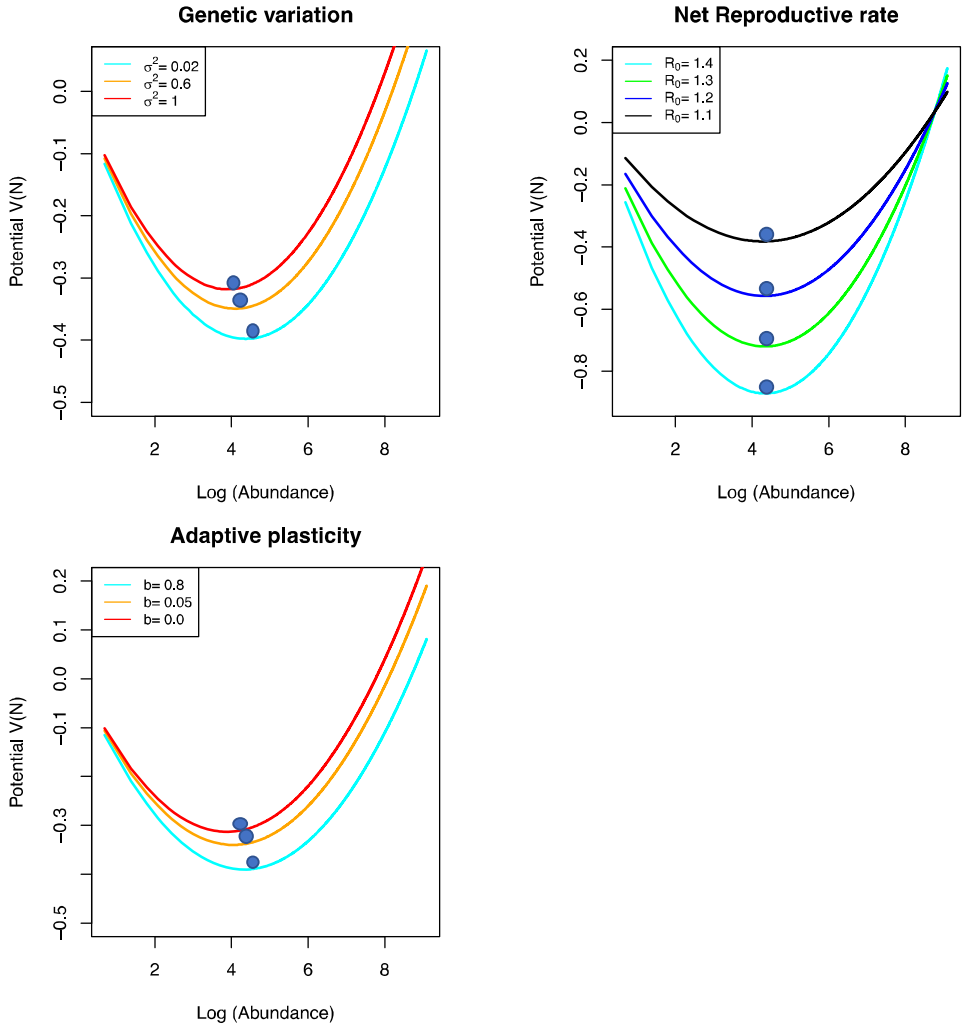

779

780

781 Figure 2.

782

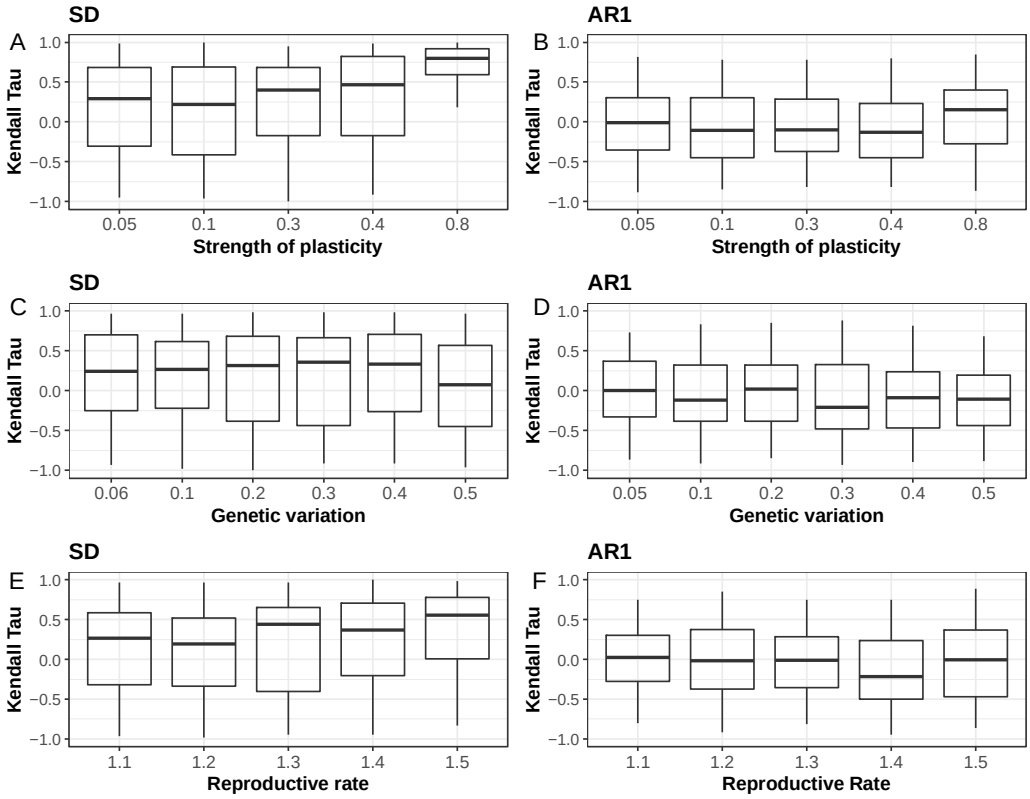

783

784 Figure 3.

785

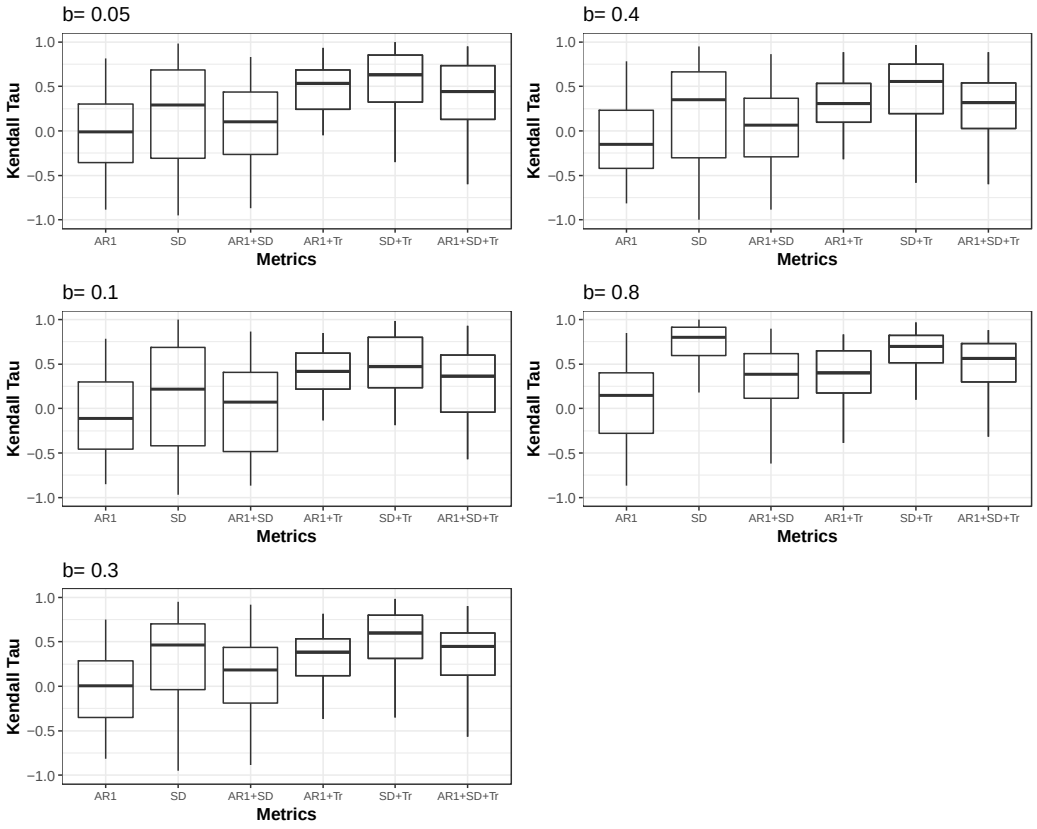

786

787 Figure. 4

788

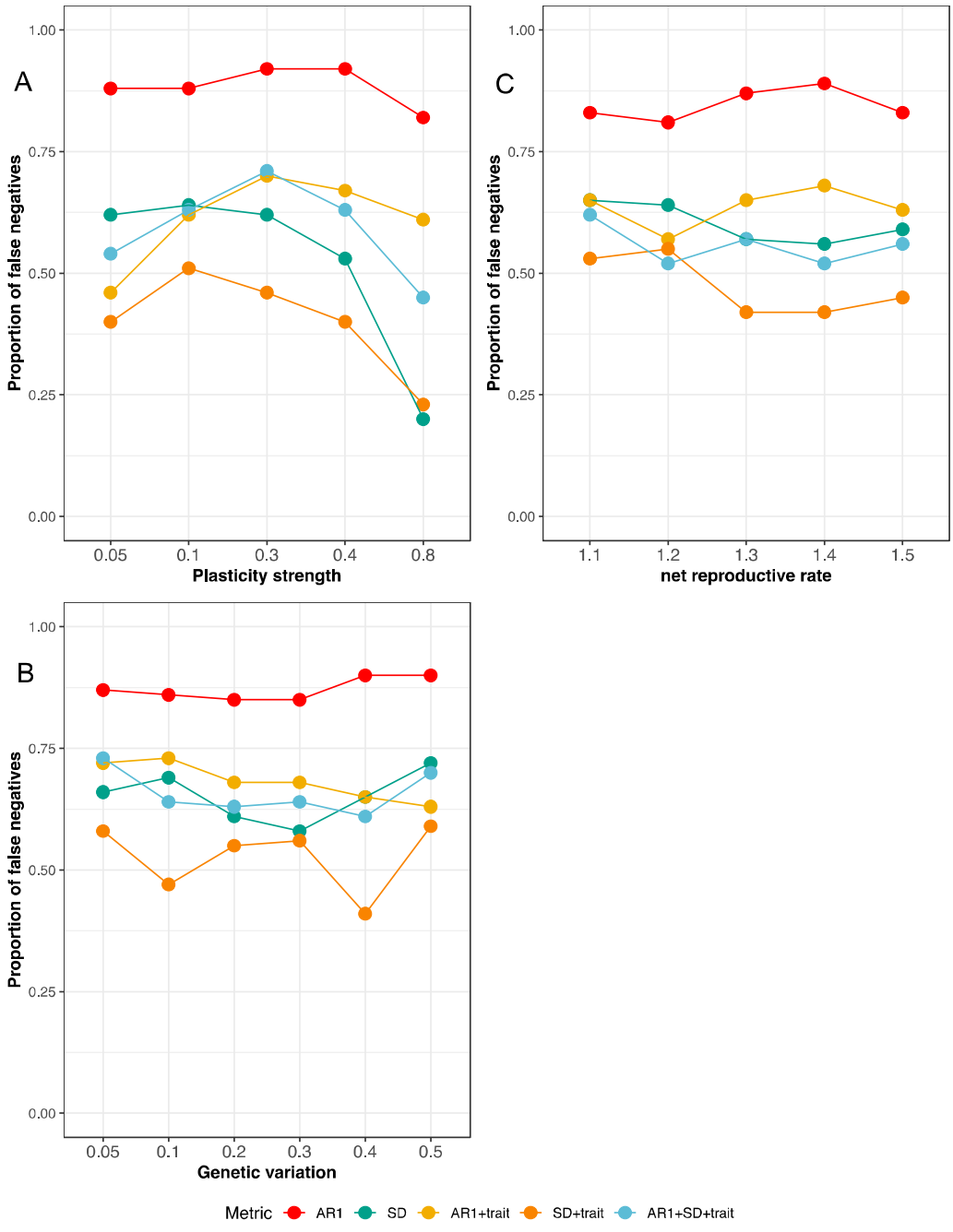

789

790 Figure 5.